Experimental and Theoretical Electron Density Study of a Highly Twisted Polycyclic Aromatic Hydrocarbon: 4-Methyl-[4]helicene

David J. Wolstenholme,*,† Chérif F. Matta,*,†,‡ and T. Stanley Cameron†

Department of Chemistry, Dalhousie University, Halifax, Nova Scotia B3H 4J3, Canada, and Department of Chemistry and Physics, Mount Saint Vincent University, Halifax, Nova Scotia B3M 2J6, Canada

Received: February 5, 2007; In Final Form: June 12, 2007

Helicenes are molecules of considerable interest in view of their aromaticity which persists despite a marked departure from planarity and because of the extreme potency of some of their metabolites as tumor and mutation promoters. In this study, the electron density of 4-methyl-[4]helicene (or 4-methylbenzo[c]-phenanthrene) is studied topologically with an emphasis on the fjord region since this region is where metabolic activation is initiated. The molecule consists of four fused aromatic rings that assume a twisted geometry. This geometry brings two hydrogen atoms into close proximity in the fjord region of the molecule accompanied by the appearance of an intramolecular C−H$^{\delta+}$···$^{\delta+}$H−C bond path (an interaction termed hydrogen−hydrogen or H− H bonding to distinguish it from dihydrogen bonding from which it is qualitatively distinct). In addition to the intramolecular H−H interaction, a number of intermolecular interactions are shown to be involved in the packing of this molecule in the crystalline state. The effect of the nonplanarity of the molecule on the local aromaticity of each ring is also discussed.

Introduction

Polycyclic aromatic hydrocarbons (PAHs) have received considerable attention because of their rich chemistry,[1−5] physical properties,[6] technological and industrial applications,[1] aromaticity,[7−16] and role as a major class of environmental pollutants and carcinogens.[17−19]

Helicenes constitute a subclass of PAHs that can possess a full turn of the helix. In this case, the title compound possesses an outline of a semicircle. Under these circumstances, there will be a highly crowded region in the vicinity of the center of the semicircle known as the fjord region of the molecule. This will cause the molecule to twist. These twisted helicenes are precursors of extremely potent mutagenic[20−22] and tumorigenic[23−28] metabolites, but literature reporting their accurately determined electron densities is scarce, possibly because they are generally difficult to crystallize. We present here an accurate low-temperature (113 K) experimental determination of the geometry of a representative molecule of a twisted helicene, 4-methyl-[4]helicene (Figure 1), followed by a determination of its experimental electron density and a comparison with theory.

The crystalline state of the title compound will be shown to contain several weak inter- and intramolecular interactions. The fjord region of the helicene molecule is a region key to the metabolic activation of these compounds[27−29] and will be shown to form a 7-membered ring due to a weak intramolecular hydrogen−hydrogen (C−H$^{\delta+}$···$^{\delta+}$H−C) bonding interaction, an interaction which is distinct from dihydrogen bonding.[30−33] [Dihydrogen bonding is symbolized by X−H$^{\delta+}$···$^{\delta-}$H−E, where the X−H group is a proton donor, such as O−H or N−H, and the E group is typically a transition metal.[34−44]Dihydrogen bonding is a subclass of hydrogen bonding where the proton acceptor happens to be another (but hydridic) hydrogen atom.]

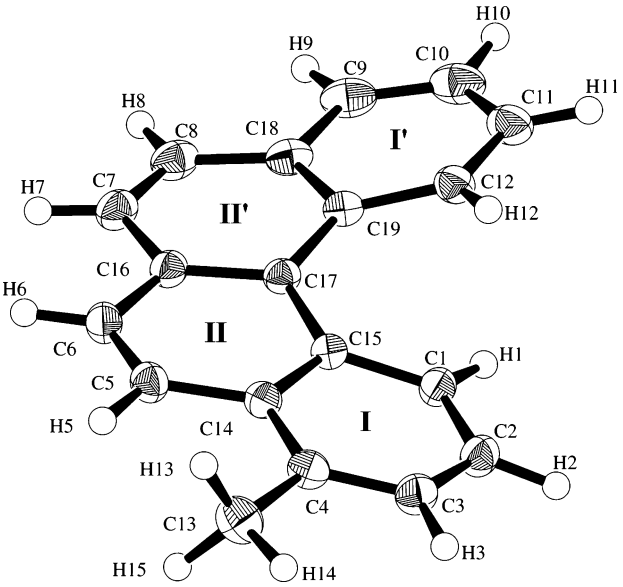

Figure 1. ORTEP diagram with labels for atoms of 4-methyl-[4]-helicene at 113 K with 50% probability ellipsoids for carbon atoms.

Hydrogen−hydrogen (or H−H) bonding is a weak, stabilizing interaction between two hydrogen atoms which carry similar or identical partial charges by symmetry.[30−33] The charges on the two interacting hydrogen atoms are often small but not necessarily of the same sign. Consequently, the H−H interaction is not dominated by electrostatic attraction as in the case of dihydrogen bonding (or hydrogen bonding in general).[33]

Overwhelming evidence of the existence of inter- and intramolecular H−H bonding interactions from experiment,[30,32,43,45−57] theory,[31,33,56−71] and chemical informatics[44] has appeared in the literature. This extensive literature report on stable H−H bonding interactions in crystals and in the gas phase but the distinction between H−H bonding and "dihydrogen bonding" is often not recognized.[31,33]

* To whom correspondence should be addressed. D.W.: phone, +1-(902)-494-3759, e-mail, dwolsten@dal.ca. C.F.M.: phone, +1-(902)-457-6142; e-mail, cherif.matta@msvu.ca.

† Dalhousie University.

‡ Mount Saint Vincent University.

10.1021/jp071002+ CCC: $37.00
Published on Web 08/17/2007

Before much of the literature on H−H bonding appeared some authors referred to these interactions as nonbonding repulsive interactions[72] despite the fact that they exist in fully optimized equilibrium geometries, i.e., stationary points on the potential-energy surfaces, where no net repulsive or attractive forces exist between atoms or nuclei. Recently, this classical view was reiterated on the basis of an arbitrary partitioning of interaction energy followed by several choices of physically unrealizable intermediate states.[73] The conclusions based on this arbitrary partitioning of the total energy have been rebutted.[74]

The present paper reports on several weak inter- and intramolecular interactions on the basis of the topology and the topography of the electron density of 4-methyl-[4]helicene (Figure 1) within the framework of the quantum theory of atoms in molecules (QTAIM).[75−79]

QTAIM extracts information on chemical bonding from the topology of the electron density distribution. This is achieved by locating the bond paths and bond critical points (BCP) for the interactions of interest. The bond path is a line in space linking the nuclei of two chemically bonded atoms where the electron density is a maximum with respect to any neighboring line and necessary for chemical bonding regardless of its nature (ionic, covalent, hydrogen, van der Waals, etc.).[80,81] The BCP is a minimum in the electron density along the bond path but a maximum in the two principal directions perpendicular to the bond path.

The type of interactions occurring in a molecular crystal can be characterized by the value of the electron density at the BCP (ρ_b), its Laplacian ($\nabla^2\rho_b$), and the interaction length (R_{ij}).[75,78,82] The density is locally concentrated when the value of $\nabla^2\rho_b$ is less than zero as in the case of shared interactions. When $\nabla^2\rho_b$ is greater than zero, the density is locally depleted as in closed-shell interactions.

In closed-shell interactions (such as van der Waals, hydrogen, or H−H bonding) the local excess in the kinetic energy is dominant, whereas in open-shell interactions (covalent/shared bonding) the lowering of the potential energy dominates.

Besides weak interactions, this work also examines the local aromaticity of the four rings of the highly twisted polycyclic aromatic title compound. It is generally observed that aromaticity is diminished in nonplanar molecules as compared with their coplanar analogues. The title compound is ideal for an examination of the effect of its departure from planarity on the local aromaticity of each of its rings.

Measures of the aromaticity of a ring in a polycondensed benzenoid have been defined using the carbon−carbon delocalization index,[83] δ(A,B).[8,9,84−87] The delocalization index provides a measure of the number of electrons delocalized or shared between two atomic basins, A and B. For a closed-shell molecule, the delocalization index between basins A and B is given by[83]

$$\delta(\mathrm{A,B}) = 2|F^{\alpha}(\mathrm{A,B})| + 2|F^{\beta}(\mathrm{A,B})| \quad (1)$$

where the Fermi correlation is defined as

$$F^{\sigma}(\mathrm{A,B}) = -\sum_i \sum_j \int_A \mathrm{d}\mathbf{r}_1 \int_B \mathrm{d}\mathbf{r}_2 \{\phi_i^*(\mathbf{r}_1)\phi_j(\mathbf{r}_1)\phi_j^*(\mathbf{r}_2)\phi_i(\mathbf{r}_2)\}$$

$$= -\sum_i \sum_j S_{ij}(\mathrm{A})S_{ji}(\mathrm{B}) \quad (2)$$

where $S_{ij}(\Omega) = S_{ji}(\Omega)$ is the overlap integral of two spin orbitals over a region Ω and σ represents spin (α or β).

TABLE 1: Experimental X-ray Data

compound formula	$C_{19}H_{14}$
cryst. size (mm)	0.18 × 0.19 × 0.27
fw (g/mol)	242.32
space group	$P2_1/c$ (no. 14)
wavelength (Å)	0.7107
a (Å)	7.5875(5)
b (Å)	11.1085(5)
c (Å)	14.9042(9)
β (deg)	92.772(3)
V (Å^3)	1246.4(3)
Z	4
μ (cm^{-1})	0.073
D_{calcd} (g/cm^3)	1.291
F(000)	512
reflns collected	20 461 ($\theta \le 90°$)
reflns (multipole)	6861
max 2θ (collection)	144.32
sin θ/λ (multipole)	1.00
$R(F)$	3.84%
$R_w(F)$	4.26%
GOF	2.061
no. of parameters	172
collection range	$-11 \le h \le 19$
	$-22 \le k \le 29$
	$-39 \le l \le 33$

Experimental Section

A colorless prismatic crystal of $C_{19}H_{14}$ of ca. 0.18 × 0.19 × 0.27 mm was mounted on a glass fiber. All measurements were made on a Rigaku RAPID area detector with graphite monochromated Mo Kα radiation. The crystal data of the X-ray diffraction experiment can be found in Table 1. The data was collected at a temperature of 113 ± 0.5 K to a maximum 2θ value of 144.32° with a total of 54 oscillation images. However, the title compound produced no measured reflections above 120.0° and only 48 very weak reflections above 105.0°. A sweep of the data was done using ω scans from 20.0° to 110.0° in steps of 5.0° at $\chi = 0.0°$ and $\Phi = 0.0°$. A second sweep was then performed using ω scans from 20.0° to 200.0° in steps of 5.0° at $\chi = 54.0°$ and $\Phi = 180.0°$. The exposure rate in both sweeps was 40.0 [min/5.0°]. The crystal-to-detector distance was fixed at 127.4 mm. Data collection was processed with d*TREK as incorporated in the CrystalClear software package,[88] while averaging and merging of the reflection intensities were performed with Sortav[89] as included in the WinGX software.[90] The structure was solved by direct methods and expanded using Fourier techniques through the CrystalStructure software.[91] Non-hydrogen atoms were refined anisotropically, and the hydrogen atoms were refined isotropically. The final cycle of full-matrix least squares was refined on F and based on 20 461 observed reflections [$I > 3.00\sigma(I)$] and 230 variable parameters. All calculations were performed using the CrystalStructure crystallographic package except for the refinements, which were performed using a SHELXL interface.[92] All of the molecular thermal ellipsoid plots were generated using the ORTEP-3 program.[93]

Multipole Refinement. For the experimental measurement and analysis of the electron density of the 4-methyl-[4]helicene crystal, the electron density was obtained through the Hansen−Coppens multipole expansion model[94] which can be expressed by the following equation

$$\rho(\mathbf{r}) = P_c\rho_{core}(\mathbf{r}) + P_v\kappa^3\rho_{valence}(\kappa\mathbf{r}) + \sum_{l=0}^{l_{max}} \kappa'^3 R_l(\kappa'\mathbf{r}) \sum_{m=0}^{l} P_{lm\pm} d_{lm\pm}(\theta,\varphi) \quad (3)$$

where ρ_{core} and $\rho_{valence}$ are spherically averaged Hartree−Fock core and valence densities, $d_{lm\pm}$ represents spherical harmonic angular functions, R_l is the radial function, κ and κ' are the expansion−contraction parameters, and P_v and $P_{lm\pm}$ represent the population parameters.

The multipole refinement was carried out with the module XDLSM incorporated in the software package XD.[95] The residual bonding density not modeled in the conventional spherical refinement was taken into account in the multipole refinement. The scattering factors used in the multipole refinement were those derived by Su and Coppens wave functions for all atoms.[96] The least-squares refinement involved minimization of the $\Sigma w(|F_0| - K|F_c|)^2$ function for all reflections with $I > 3\sigma(I)$. The multipole refinement was carried out with a sin θ/λ limit of 1.0 since the reflections greater than this cutoff were very weak and fell into the realm of the background. The multipole expansion was applied up to the octapole level ($l_{max} = 3$) for all carbon atoms and up to the dipole level ($l_{max} = 1$) for all hydrogen atoms. The κ and κ' parameters were employed for four subsets of carbons until a reasonable model was achieved. The expansion/contraction parameters of the hydrogen atoms were left fixed at the default XDLSM value of 1.2. In order to determine accurate positional and thermal parameters for the carbon atoms, a high-order (sin $\theta/\lambda \geq 0.6$) refinement was performed. A low-order (sin $\theta/\lambda \leq 0.6$) refinement was then performed in order to obtain accurate positional and thermal parameters for hydrogen atoms. The carbon−hydrogen bond lengths were then set to the reported neutron diffraction distance for the rest of the multipole refinement (C_{ar}−H = 1.083).[97,98] The charge neutrality constraint was applied throughout the multipole refinement in order to achieve an overall neutral molecule. The multipole refinement strategy used was as follows: (a) scale factor, (b) P_{lm} for all atoms, (c) κ and κ' for all carbon atoms, (d) P_v for all atoms, (e) positional and thermal parameters for all carbon atoms. This procedure was cycled through until convergence was achieved. The difference mean-square displacement amplitudes (DMSDA) for all bonds were within the Hirshfeld limits.[99] Evidence for the good quality of the final model is presented in residual maps in select planes of 4-methyl-[4]helicene (Supporting Information). The XDPROP program incorporated into the XD package[95] was then used to determine the total electron density, $\rho(\mathbf{r})$, the Laplacian, and the ellipticity for all C−H$^{\delta+}\cdots^{\delta+}$H−C interactions along with the other interactions. All static, residual, dynamic, and deformation maps were produced using the XDGRAPH option in the XD package. All experimental atomic basin parameters were determined using the TOPXD program incorporated in the XD package.[95] The final atomic coordinates, thermal parameters, bond lengths, and angles for the 4-methyl-[4]helicene molecule are provided as Supporting Information.

Computational Method. An unconstrained geometry optimization of a 4-methyl-[4]helicene molecule was performed at the B3LYP/6-31++G(d,p) level of theory starting from the experimental geometry, and a "wave function" was obtained at the same level of theory. The electron density was integrated over atomic basins according to the quantum theory of atoms in molecules[75−79] using PROAIM,[100−102] and the BCP data and the molecular graph were obtained using AIM 2000.[103,104] AIMDELOC[105] was used to calculate the delocalization indices[83] δ(A,B) between the atoms from the atomic overlap matrices.

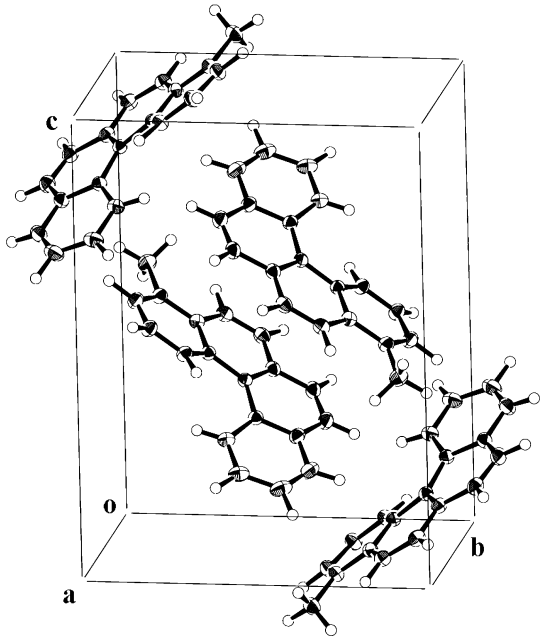

Figure 2. Packing diagram of 4-methyl-[4]helicene showing all the symmetry-related molecules in the unit cell.

Schleyer's nucleus independent chemical shifts (NICS)[106−108] were obtained by calculating the magnetic shielding (in ppm) at the centroid of each of the four aromatic rings.

Tight convergence thresholds were imposed on the geometry optimization. The final maximum force and root-mean-square (rms) of the forces were as small as 0.000021 and 0.000004 hartrees/bohr, respectively. Atomic integrations were performed with a high numerical precision as revealed by the following:[82] (1) the sum of the integrated atomic populations $N(\Omega)$ differ from the molecular value of 128 e by 0.0033 e; (2) the sum of the atomic energies differs from the molecular value of −732.532472 au by 0.15 kcal/mol; (3) the average integrated magnitude of the atomic Laplacian $|L(\Omega)|$ was 0.00015-($\pm$0.00019) au with a maximum of 0.00082 au.

Results and Discussion

Crystal Packing. 4-Methyl-[4]helicene crystallizes with four molecules in the unit cell (Figure 2), which allows for several weak inter- and intramolecular interactions to be formed. The weak intermolecular interactions between neighboring symmetry-related molecules appears to play an important role in formation of the crystal. A total of 13 inter- and 1 intramolecular closed-shell interaction bond paths were found in this crystal and are characterized on the basis of the bond critical point properties. The C−H···C (Figure 3a) and C−H···H−C (Figure 3b) weak intermolecular interactions are all accompanied by bond paths with bond lengths ranging from 2.167 to 2.992 Å, consistent with weak van der Waals interactions or H−H bonding.

Intramolecular H−H Bond Path in the Fjord Region. A close H···H contact between H(1) and H(12) occurs in the crowded fjord region of the molecule where the nuclei of these two hydrogen atoms are separated by 1.938 Å in the experimental geometry and by 1.985 Å in the optimized geometry, values that are significantly shorter than twice the van der Waals radius of the hydrogen atom (2.4 Å). The experimentally and theoretically determined intramolecular bond paths are shown in Figures 3c and 4, respectively. In both figures an intramolecular bond path links H(1) to H(12) in the fjord region of the

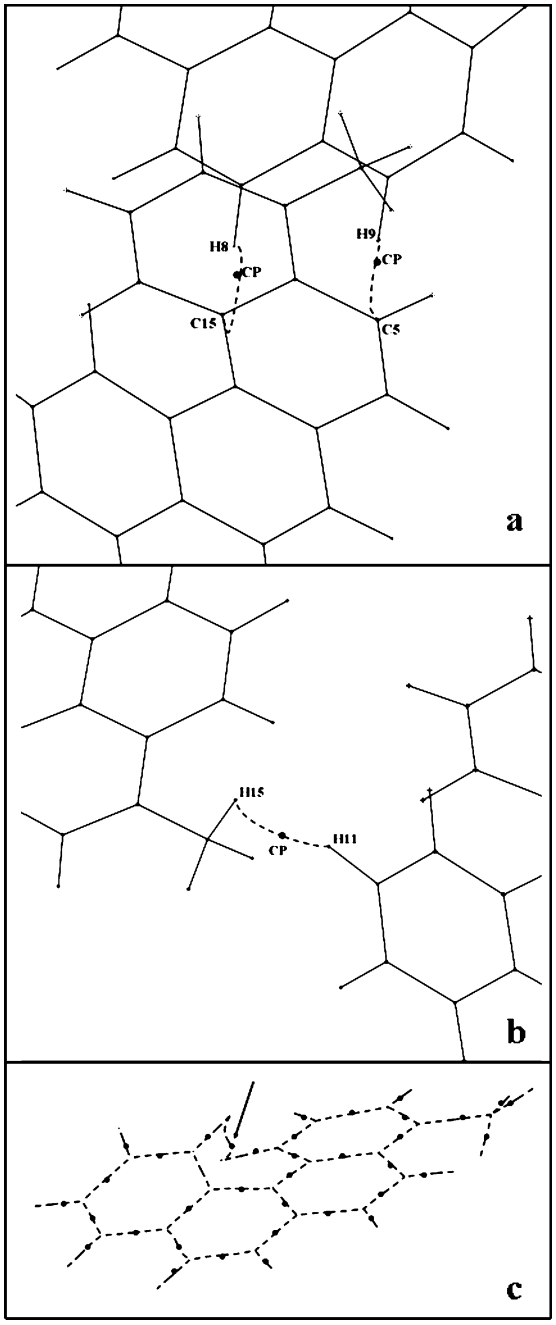

Figure 3. Bond paths in 4-methyl-[4]helicene with the positions of the bond critical point locations indicated along the C−H···C, C−H$^{\delta+}$···$^{\delta+}$H−C, C−C, and C−H bond paths: (a) intermolecular C−H···C interactions are traced with dashed lines, (b) intermolecular C−H···H−C interaction is traced with a dashed line, and (c) all the intramolecular C−C, C−H, and H−H bond paths are traced with dashed lines.

helicene. Since this closed-shell bond path exists in an equilibrium geometry and is shared between two similar atoms, this interaction can be classified as a hydrogen−hydrogen bonding. The bond path lengths of this intramolecular H−H bonding are 2.107 (exp) and 2.176 Å (theory). The experimental and calculated bond paths are considerably curved since they are 0.169 and 0.191 Å longer than the internuclear distances, a curvature often exhibited by weak closed-shell bonding.

In a series of closely related 1,12-difluoro[4]helicenes, a bond path links the two proximal fluorine atoms also closing a 7-membered ring in the fjord region of the molecule.[109,110] In the case of the fluorine substituents, however, the departure of

TABLE 2: Key Proper and Improper Dihedral Angles Specifying the Overall Molecular Geometry of [4]Helicenes

dihedral angle	experimental	theoretical	1,12-fluorinated derivative (theor.)[a]
C1−C15−C19−C12	−28.6	−31.8	−41.4
C2−C14−C18−C11	−23.7	−28.2	−35.6
C3−C4−C9−C10	−21.0	−26.4	−33.4
average[b]	−24.4	−28.8	−36.8
C1−C15−C17−C19 (δ)	−15.7	−19.2	−25.2
C12−C19−C17−C15 (δ')	−18.7	−18.9	−24.9
C2−C6−C7−C11	−16.2	−21.3	−26.7

[a] 4-Methyl-1,12-difluoro[4]helicene, the difluorinated derivative of the title compound [unpublished data from a geometry optimization at the B3LYP/6-31G(d) level of theory and discussed in refs 109 and 110]. [b] The average of the three angles above it (this average specifies the approximate mean angle between rings I and I′).

planarity of the carbon skeleton is so severe (Table 2) that the ring surface splits into two ring surfaces, resulting in the appearance of two (rather than one) ring critical points in the 7-MR.[109] As required by the Poincaré−Hopf relationship,[75] this extra ring critical point in fluorinated helicenes is accompanied by the appearance of a cage critical point in a single ring.[109] The 1,12-unsubstituted helicene considered in the present study is insufficiently twisted to give rise to the unusual topology exhibited by the fluorinated derivatives [the dihedral angle between rings I and I′ is −24° and −29° in the experimental and theoretical structures, respectively, while in the fluorinated derivative the theoretical value is −37° (Table 2)].

Properties of the Electron Density at the BCP for the Weak Closed-Shell Interactions. The values of the electron density at the BCP, ρ_b, for all closed-shell inter- and intramolecular interactions in the crystal of 4-methyl-[4]helicene are relatively small (Table 3). The largest ρ_b for these weak interactions belongs to the intramolecular H−H bonding closing the 7-MR in the fjord region of the molecule. The ρ_b values for the C−C bonds in the aromatic ring system are naturally much larger and range from 1.863 to 2.277 e Å^{-3} (Table 4), while ρ_b for the C−C$_{Me}$ bond is somewhat smaller, 1.713 e Å^{-3}. In all of the weak inter- and intramolecular interactions, the $\nabla^2\rho_b$ values are small and positive, as expected for closed-shell interactions. The Laplacian maps for each of these interactions show a region of charge depletion accompanied by a (3,−1) critical point, which is characteristic of these weak closed-shell interactions (Figure 5a,b). In contrast, all the C−C bonds possess large negative $\nabla^2\rho_b$ values and clearly exhibit bonding charge concentration in the Laplacian contour map (Figure 5c).

The mutual penetration of the donor and acceptor atoms for each weak inter- and intramolecular interaction shows that the van der Waals spheres of these atoms are overlapping significantly for five interactions (two C−H$^{\delta+}$···$^{\delta+}$H−C and three C−H···C), resulting in a positive $\Delta r_A + \Delta r_B$ value. The Δr_X terms simply represent the nonbonding radius of the acceptor/donor atom minus its bonding radius (the nonbonding radius of the carbon atoms is taken as 1.85 Å and that of the hydrogen atoms as 1.2 Å,[95] values that represent the gas-phase van der Waals radius for each atom).[111] The bonding radius is taken as the distance from the nucleus to the BCP. Not surprisingly, the largest mutual penetration occurs for the intramolecular H−H bond in the fjord region of the molecule (0.293 Å).

Properties of the Electron Density at the BCP for the Carbon−Carbon Bonds. The range of bond properties in the carbon ring system is typical of aromatic compounds as can be gleaned from Table 4 by comparison with the corresponding

TABLE 3: Properties of the Bond Critical Points for the Weak Interactions

interaction	ρ_b (e Å^{-3})	$\nabla^2\rho_b$ (e Å^{-5})	R_{ij} (Å)	$\Delta r_A + \Delta r_B$ (Å)	$\Delta r_A - \Delta r_B$ (Å)
		intramolecular (C−H···H−C)			
H(1)−H(12)[a]	0.149	1.572	1.976	0.425	0.022
	0.105	1.626	1.985	0.224	0.003
		intermolecular (C−H···H−C)			
H(1)−H(5)$^{(-1+x,+y,+z)}$	0.026	0.420	2.474	−0.074	0.055
H(2)−H(13)$^{(-1+x,+y,+z)}$	0.015	0.337	2.512	−0.112	0.177
H(8)−H(12)$^{(+1-x,1/2+y,1.5-z)}$	0.024	0.421	2.583	−0.183	0.267
H(9)−H(11)$^{(-x,1/2+y,1.5-z)}$	0.017	0.226	2.904	−0.504	−0.117
H(10)−H(12)$^{(-x,1/2+y,1.5-z)}$	0.017	0.313	2.601	−0.201	−0.222
H(11)−H(15)$^{(+x-1,1.5-y,1/2+z)}$	0.040	0.816	2.143	0.257	0.199
		intermolecular (C···H−C)			
C(2)−H(7)$^{(+1-x,+1-y,+1-z)}$	0.025	0.303	3.106	−0.056	−0.073
C(5)−H(9)$^{(+1-x,1/2+y,1.5-z)}$	0.047	0.607	2.757	0.293	−0.099
C(8)−H(14)$^{(-x,+1-y,-z)}$	0.018	0.263	3.209	−0.159	0.045
C(10)−H(7)$^{(-1+x,+y,+z)}$	0.030	0.358	3.143	−0.093	−0.176
C(11)−H(3)$^{(+x,1.5-y,1/2+z)}$	0.038	0.500	2.969	0.081	−0.014
C(11)−H(6)$^{(-1+x,+y,+z)}$	0.016	0.253	3.150	−0.100	0.077
C(15)−H(8)$^{(+1-x,1/2+y,1.5-z)}$	0.029	0.449	2.979	0.071	0.077

[a] First and second lines list experimental and theoretical values, respectively.

values of the bond properties calculated for benzene at the same level of theory. Furthermore, there are more significant fluctuations in the bond properties of the substituted ring (ring I) when compared with its unsubstituted counterpart (ring I′) (see Figure 1). We can expect, therefore, a reduction in the aromaticity of ring I when compared with I′ as will be seen in a later section. The effect of the substitution is diluted when rings II and II′ are compared, which exhibit more similarities when the equivalent bonds are compared (Table 4).

Molecular Electrostatic Potential. The electrostatic potential (ESP), $V(\mathbf{r})$, can be calculated from the electron density according to the equation

$$V(\mathbf{r}) = \sum_A \frac{Z_A}{|\mathbf{R}_A - \mathbf{r}|} - \int \frac{\rho(\mathbf{r}')}{|\mathbf{r}' - \mathbf{r}|} d\mathbf{r}' \qquad (4)$$

where Z_A is the charge of nucleus A having a position vector $\mathbf{R}_A$ and $\rho(\mathbf{r}')$ is the electron density. The partitioning of the electron density as a multipole expansion allows the direct space calculation of the ESP distribution.[112]

The molecular electrostatic potential maps carry a wealth of quantitative and qualitative information about the molecule (Figure 6). These figures clearly show a nucleophilic region sandwiching the π-system, leaving a more electrophilic region in the plane of the hydrogen atoms. The molecule packs in the crystal so that the aromatic plane of a molecule is approximately perpendicular to the aromatic planes of two of its neighbors and displaced sidewise with respect to two other neighbors, bringing the positive regions of the hydrogen atoms (the aromatic and the methyl hydrogen atoms) in contact with the electron-rich aromatic system (see Figure 2). It is also interesting to note that both experimental (Supporting Information) and theoretical maps show a region of positive electrostatic potential in the fjord region of the molecule, which includes the intramolecular H−H bond path.

Atomic Properties of the Hydrogen Atoms. Table 5 lists a set of properties for the atoms in 4-methyl-[4]helicene obtained from experiment and the corresponding values calculated at the B3LYP/6-31++G(d,p)//B3LYP/6-31++G(d,p) level of theory. The listed atomic properties are the charges $q(\Omega)$ in au, the total atomic energies $E(\Omega)$ in au, the atomic energies relative to the energies of the corresponding free isolated ground state atom [C($^3P_0$) and H($^2S_{1/2}$)] $E_{Rel}(\Omega)$ in kcal/mol, and the atomic volumes in au integrated up to the outer 0.001 au isosurface. [Trends in atomic energies calculated using Kohn−Sham "wave functions" have been previously found to parallel Hartree−Fock and MP2 levels of theory even when self-consistent virial scaling (SCVS) is included in these latter calculations.][31]

The theoretical results listed in Table 5 show that the two hydrogen atoms involved in the intramolecular H−H bonding are the most stable hydrogen atoms in the isolated molecule, each being (on average) more stable than the remaining 12 hydrogen atoms by ca. 3.7 kcal/mol. If we exclude the three methyl hydrogen atoms from the averaging and call the hydrogen atoms of the ring system "normal hydrogen atoms" (hydrogen atoms numbered from 2 to 11), H(1) and H(12) are found to be 4.2 and 3.6 kcal/mol more stable than the normal hydrogen atoms, respectively. Since the major part of the stabilization of the hydrogen atoms involved in the intramolecular H−H bond arises from formation of the H−H interatomic zero-flux surface,[31,33] the *local* stabilization energy of this H−H bonding interaction is estimated to ca. 7−8 kcal/mol.

From Table 5, the theoretical volumes of the two hydrogen atoms involved in the intramolecular H−H bond are consistent with previous findings.[31,33] They have significantly smaller volumes than either the methyl or the 'normal' hydrogen atoms of the aromatic system. The calculated volumes of the two hydrogens H(1) and H(12) are ca. 6.0 au smaller than the average of the rest of the hydrogen atoms in this molecule (49.8 ± 0.9 au). Most of the experimental volumes associated with the hydrogen atoms are in good agreement with those of the theoretical calculations. The small (but more significant) deviations of some experimental atomic volumes from the corresponding theoretical values are the result of intermolecular weak hydrogen bonds or H−H bonds, interactions that only exist in a crystal and are absent in the gas-phase calculations.

Finally, both the theoretical and experimental results listed in Table 5 show that the hydrogen atoms in this compound all carry small atomic charges as expected in a hydrocarbon. The differences in the signs associated with some of the hydrogen atom charges is commonly observed between the atomic charges obtained from the experimental multipole refinement and those obtained from theoretical calculation of the isolated molecule.[113,114]

TABLE 4: Properties of the Bond Critical Points for All the Carbon−Carbon Bonds

bond[a]	$\delta(A,B)$[b]	ρ_b (e Å^{-3})	$\nabla^2\rho_b$(e Å^{-5})	ϵ	R_{ij} (Å)
$(CC)_{benzene\ (theor.)}$[c]	1.389	2.100	−20.432	0.202	1.398
C(1)−C(2)	1.480	2.223	−20.805	0.230	1.379
	1.463	2.166	−21.511	0.235	1.380
C(1)−C(15)	1.238	1.982	−16.286	0.230	1.422
	1.268	2.010	−18.779	0.168	1.422
C(2)−C(3)	1.336	2.085	−18.305	0.170	1.408
	1.309	2.065	−19.988	0.174	1.408
C(3)−C(4)	1.414	2.161	−19.068	0.240	1.383
	1.437	2.157	−21.191	0.241	1.385
C(4)−C(13)	1.013	1.713	−12.520	0.080	1.504
	1.011	1.703	−14.304	0.030	1.512
C(4)−C(14)	1.263	2.009	−17.047	0.210	1.428
	1.239	1.983	−18.246	0.166	1.431
C(5)−C(6)	1.541	2.277	−21.253	0.250	1.365
	1.537	2.231	−22.686	0.263	1.365
C(5)−C(14)	1.179	1.917	−14.792	0.210	1.431
	1.208	1.984	−18.525	0.140	1.431
C(6)−C(16)	1.247	1.992	−17.176	0.180	1.429
	1.208	1.996	−18.813	0.140	1.428
C(7)−C(8)	1.480	2.223	−19.962	0.300	1.362
	1.547	2.238	−22.796	0.269	1.363
C(7)−C(16)	1.269	2.016	−16.859	0.190	1.429
	1.201	1.983	−18.577	0.137	1.431
C(8)−C(18)	1.309	2.057	−17.701	0.050	1.435
	1.202	1.991	−18.737	0.136	1.430
C(9)−C(10)	1.331	2.080	−16.831	0.210	1.376
	1.464	2.169	−21.588	0.234	1.380
C(9)−C(18)	1.215	1.957	−14.775	0.190	1.418
	1.271	2.006	−18.698	0.169	1.418
C(10)−C(11)	1.348	2.097	−18.317	0.160	1.410
	1.310	2.059	−19.845	0.173	1.409
C(11)−C(12)	1.401	2.149	−19.501	0.200	1.384
	1.458	2.153	−21.253	0.232	1.384
C(12)−C(19)	1.284	2.031	−18.195	0.220	1.423
	1.273	2.006	−18.698	0.169	1.422
C(14)−C(15)	1.310	2.058	−17.642	0.140	1.432
	1.237	1.965	−17.854	0.163	1.437
C(15)−C(17)	1.186	1.925	−14.643	0.270	1.454
	1.172	1.885	−16.676	0.136	1.457
C(16)−C(17)	1.253	1.999	−16.828	0.210	1.415
	1.296	2.231	−22.686	0.263	1.418
C(17)−C(19)	1.133	1.863	−14.533	0.250	1.458
	1.168	1.881	−16.626	0.135	1.458
C(18)−C(19)	1.226	1.969	−16.078	0.370	1.424
	1.234	1.975	−18.091	0.158	1.435

[a] The first and second lines for each row list the experimental and theoretical values, respectively. [b] The "experimental" delocalization indices were calculated using the experimental ρ_b values and the exponential regression equation obtained using the theoretical ρ_b values. [c] Bond properties for a gas-phase benzene molecule calculated at the same level of theory for comparison.

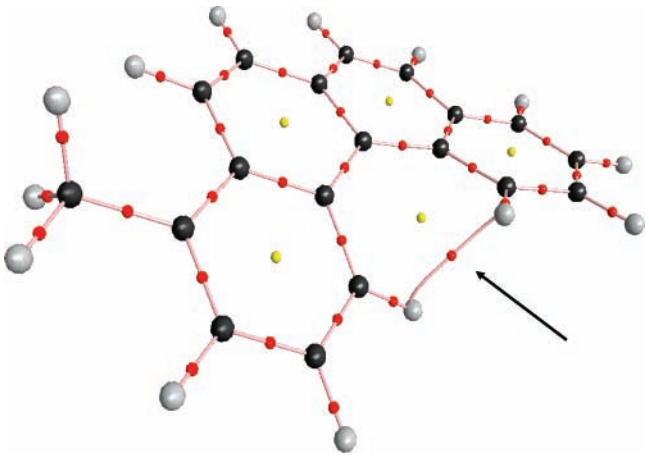

Figure 4. Molecular graph of 4-methyl-[4]helicene calculated at the B3LYP/6-31++G(d,p)//B3LYP/6-31++G(d,p) level. The bond critical point and associated bond path of the H−H bonding interaction are indicated by the arrow.

Atomic Properties of the Carbon Atoms. The experimental and theoretical results listed in Table 5 show that all carbon atoms bear small charges. As is the case for the hydrogen atoms, a generally good agreement is found between the experimental and theoretical values. The methyl carbon possesses the largest positive charge in both the experimental (q[C(13)] = 0.1415 au) and theoretical (q[C(13)] = 0.071 au) densities. The electronic charge gained by the methyl hydrogen atoms in the molecule comes in part from the methyl carbon atom C(13), where the methyl group as a whole carries a net charge of +0.0410 (theory) and +0.0517 au (experiment). This implies that the aromatic system in the isolated molecule gains electronic charge from the methyl group. In the isolated molecule, the sum of all the charges for all atoms in rings I and II, excluding the methyl substituent, results in a charge of −0.0414 au, a value almost exactly equal to the electronic charge lost by the methyl substituent. Addition of the net charges of rings I and II to that of the methyl group results in a near cancellation with a total charge of −0.0006 au. In the crystal, the sum of the charges is −0.0057 au, significantly less than that of the methyl substituent.

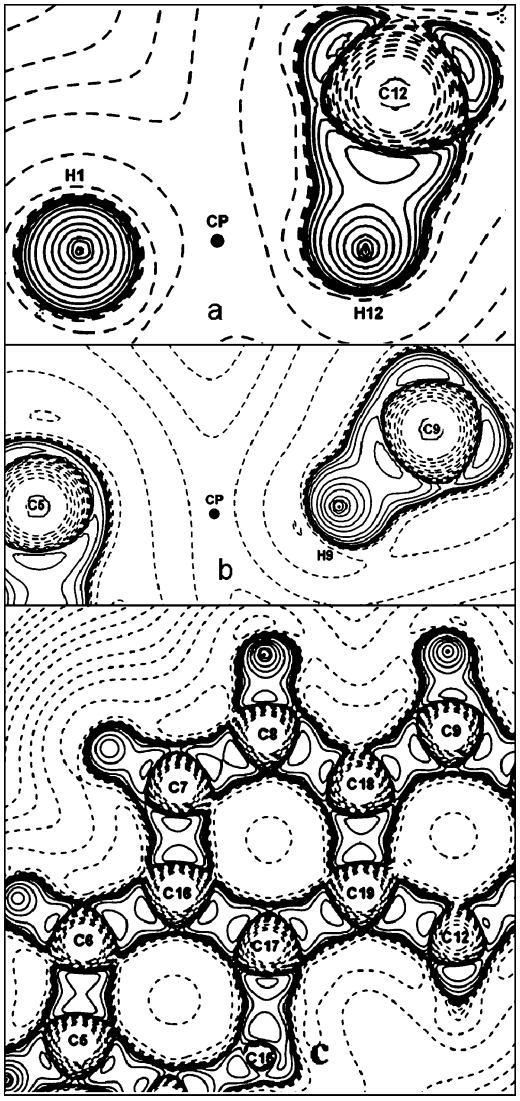

Figure 5. Experimental Laplacian maps for 4-methyl-[4]helicene showing the (3,−1) critical point in the Laplacian field. (a) Laplacian map of the intramolecular H−H interaction in the fjord region of the molecule showing the (3,−1) critical point. (b) Laplacian map of one of the intermolecular C−H···C interactions in 4-methyl-[4]helicene showing the (3,−1) critical point. (c) Laplacian map of a section of the 4-methyl-[4]helicene ring system. All solid lines represent positive charge accumulation, and all dashed lines represent charge depletion.

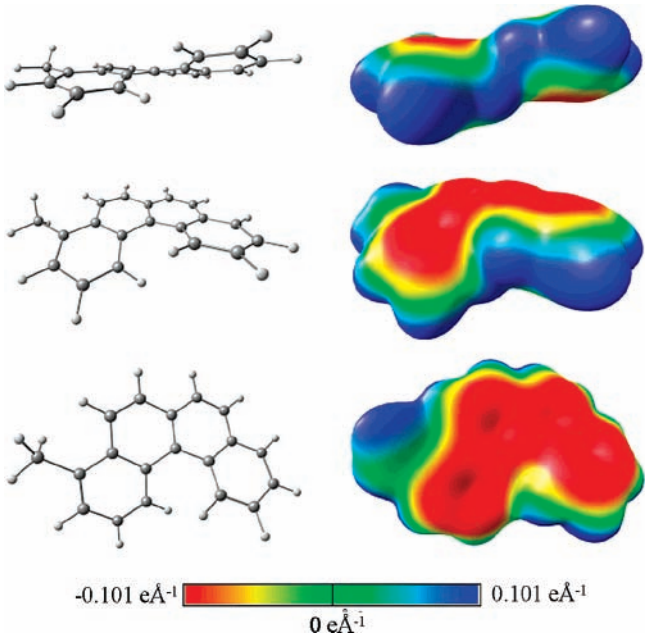

Figure 6. Molecular electrostatic potential mapped on the $\rho(\mathbf{r}) = 0.001$ au = 0.00675 e Å^{-3} isodensity surface in the range from −0.101 (red) to +0.101 e Å^{-1} (blue) in the three different orientations shown on the left calculated at the B3LYP/6-31++G(d,p) level of theory.

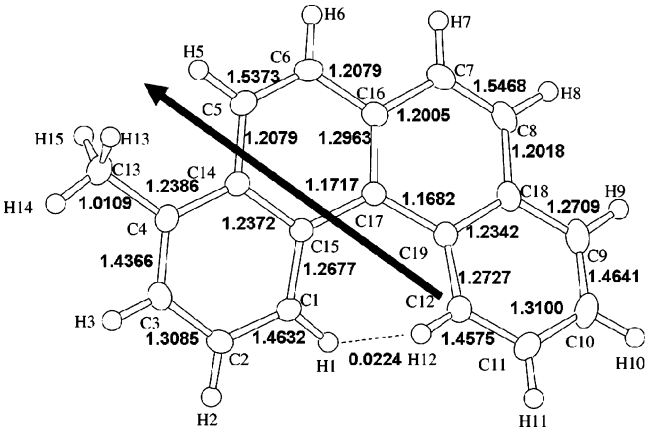

Figure 7. Diagram showing the theoretical delocalization indices values for every carbon−carbon and the hydrogen−hydrogen bond in 4-methyl-[4]helicene. The arrow represents the direction of the polarization of the molecule.

The sum of the atomic charges for all the atoms in rings I′ and II′ is −0.0065 au for the isolated molecule, an order of magnitude less negative than the corresponding moiety consisting of rings I and II (without the methyl). [Note that atoms C(16) and C(17) are included in both counts since they are parts of the two ring systems]. In the experimental calculations, the total charge of rings I′ and II′ is −0.0631 au, a value almost exactly equal to the electronic charge lost by the methyl substituent. Thus, the charge donated by the methyl is mainly localized in the two rings I and II with almost no charge leaking to the other half of the molecule in the gas-phase state. While in the crystal, the charge donated by the methyl group is mainly localized in the unsubstituted rings of a symmetry related molecule as a result of intermolecular charge transfer. This is illustrated in the packing of the molecules (Figure 2), which shows the methyl groups of one molecule pointing directly toward ring I′ of another molecule.

The magnitude of the atomic charges in rings I and II exhibit an alternation with larger magnitudes at the ortho and para positions with respect to the methyl. For example, to three decimal places, $q[C_{para}(1)] = -0.010$ au (theory)/−0.035 au (experimental) > $q[C_{ortho}(3)] = -0.009$ au (theory)/−0.030 au (experimental) > $q[C_{meta}(2)] = -0.006$ au (theory)/−0.015 au (experimental), consistent with a simple hyperconjugation resonance mechanism[115] involving the methyl hydrogen atoms.

Local Aromaticity. Solà et al.[8] found that despite the significant departure from planarity in helicene rings they tend to lose very little aromaticity when compared with their planar acenes or phenacenes counterparts. These authors also remark that there is an alternation in aromaticity from one ring to the next, the peripheral rings displaying maximal aromaticity as measured by three indices: HOMA,[116,117] NICS,[106−108] and FLU.[85,86]

We calculated three aromaticity indices, HOMA, NICS, and θ,[87] for the title compound (Table 6). The values listed in Table 6 are consistent with the values listed for HOMA and NICS in the related symmetric compound [4]helicene (and calculated at

TABLE 5: Atomic Properties: Charges $q(\Omega)$, Energies $E(\Omega)$, Relative Atomic Energies $E_{Rel}(\Omega)$, and Volumes Vol.(Ω)[a]

		$q(\Omega)$				Vol.(Ω)	
		theor.	exptl.	$E(\Omega)$	$E_{Rel}(\Omega)$[b]	theor.	exptl.
				fjord region H−H-bonded hydrogen atoms			
H	1	0.0115	0.0100	−0.63456	−83.39	43.80	38.00
H	12	0.0139	0.0243	−0.63353	−82.74	43.78	38.20
				normal hydrogen atoms			
H	2	0.0023	0.0104	−0.62727	−78.82	50.33	42.78
H	3	−0.0041	0.0219	−0.63019	−80.65	50.01	40.97
H	5	0.0035	−0.0108	−0.63194	−81.75	46.80	40.84
H	6	0.0010	0.0163	−0.62779	−79.14	50.04	41.05
H	7	0.0024	−0.0029	−0.62702	−78.66	49.97	44.00
H	8	0.0034	−0.0017	−0.62628	−78.20	50.13	40.97
H	9	0.0009	0.0023	−0.62748	−78.95	50.06	43.34
H	10	0.0052	−0.0119	−0.62574	−77.86	50.15	43.27
H	11	0.0035	0.0206	−0.62686	−78.56	50.16	44.26
				methyl hydrogen atoms			
H	13	−0.0085	−0.0436	−0.62767	−79.07	50.07	43.61
H	14	−0.0122	−0.0099	−0.63102	−81.17	49.80	43.82
H	15	−0.0092	−0.0363	−0.62832	−79.47	50.10	44.49
				carbon atoms			
C	1	−0.0103	−0.0345	−38.10274	−157.76	80.10	81.86
C	2	−0.0059	−0.0151	−38.08509	−146.68	83.85	84.14
C	3	−0.0094	−0.0299	−38.09474	−152.74	82.73	83.20
C	4	−0.0011	0.0780	−38.09187	−150.94	70.44	68.56
C	5	−0.0108	0.0032	−38.10335	−158.14	82.18	82.94
C	6	−0.0066	−0.0393	−38.10070	−156.48	82.37	86.68
C	7	−0.0065	0.0033	−38.09824	−154.94	82.40	82.53
C	8	−0.0050	−0.0258	−38.09959	−155.79	82.56	80.90
C	9	−0.0070	−0.0655	−38.09089	−150.33	82.63	84.27
C	10	−0.0021	0.0089	−38.07940	−143.11	83.75	83.31
C	11	−0.0041	0.0242	−38.07880	−142.74	83.94	84.17
C	12	−0.0080	−0.0383	−38.09795	−154.76	79.74	81.63
C(Me)	13	0.0707	0.1415	−38.00639	−97.30	67.19	70.47
C	14	−0.0032	−0.0145	−38.10624	−159.95	70.23	70.82
C	15	−0.0043	0.0466	−38.08726	−148.05	70.32	70.23
C	16	0.0048	−0.0115	−38.11986	−168.50	69.50	69.83
C	17	−0.0086	−0.0365	−38.08178	−144.60	71.02	71.89
C	18	0.0055	0.0495	−38.11445	−165.11	69.75	70.09
C	19	−0.0047	−0.0021	−38.08724	−148.03	70.41	69.76
	sum	−0.0033	0.0308	−732.5322		2150.31	2066.88
	SCF	−0.0000		−732.5325			
	diff.	0.0026		0.14724	kcal/mol		

[a] All entries are in atomic units except the relative atomic energies which are listed in kcal/mol. [b] Relative energies in kcal/mol with respect to the energies of the free isolated ground state atoms which at the B3LYP/6-31++G(d,p) level of theory are: $E[C(^3P_0)] = -37.851335$ au, and $E[H(^2S_{1/2})] = -0.501666$ au.

TABLE 6: Aromaticity Indices Calculated for the Four Rings of 4-Methyl-[4]helicene

		NICS			
ring	HOMA	GIAO	IGAIM	CSGT	θ
I	0.814	−8.110	−10.589	−10.593	0.785
II	0.578	−6.722	−8.821	−8.825	0.661
II′	0.569	−6.543	−8.721	−8.725	0.654
I′	0.853	−8.418	−11.064	−11.068	0.804

a lower level of theory, B3LYP/6-31G(d)),[85] where the peripheral rings have a HOMA index of 0.806 and a NICS of −9.99 ppm while the inner ones have a HOMA of 0.503 and a NICS of −7.62 ppm. Table 6 shows all measures of aromaticity yield a consistent picture with the local aromaticity ordering I′ > I > II > II′.

The substituted peripheral ring (I) is less aromatic than the unsubstituted one (I′) as anticipated based on the higher fluctuation of bond properties around the ring. This reduction of aromaticity is, possibly, a reflection of the uneven redistribution of charge (charge alternation) and the alternation in electron delocalization indices between bonded atoms forming ring I (when compared with the unsubstituted ring I′).

Figure 7 shows the δ(C,C′) for all the C−C bonds and δ(H1,H12) for the intramolecular H−H bond. The δ(C,C′) for the phenyl C−C bonds range from 1.1682 to 1.5468. The δ(C,C′) associated with the $C_{phenyl}-C_{methyl}$ bond is 1.0109, which is to be expected for a single C−C bond. The H−H bond has a δ(H1,H12) value of 0.0224, which is much smaller than those of the C−C bonds but still represents an appreciable amount of electron pair sharing for such a weak interaction. The arrow in Figure 7 represents the molecular dipole moment vector which points its positive side in the direction of the methyl substituent.

It has recently been shown that the experimental electron density at the BCP (ρ_b) can be correlated to the calculated delocalization indices (δ(C,C′)).[57] This signifies a correlation between experimental one-electron density (diagonal elements) and a quantity based on the full density matrix. This allows for a direct comparison of the C−C bond order to the experimental and theoretical electron densities at the BCPs. Figure 8 represents an exponential ($\delta(C,C') = \exp[A(\rho_b - B)]$) relationship between the experimental and theoretical ρ_b (both represented in e$Å^{-3}$) against the δ(C,C′). The experimental fitting parameters A and B have values of 0.7572 and 1.6990,

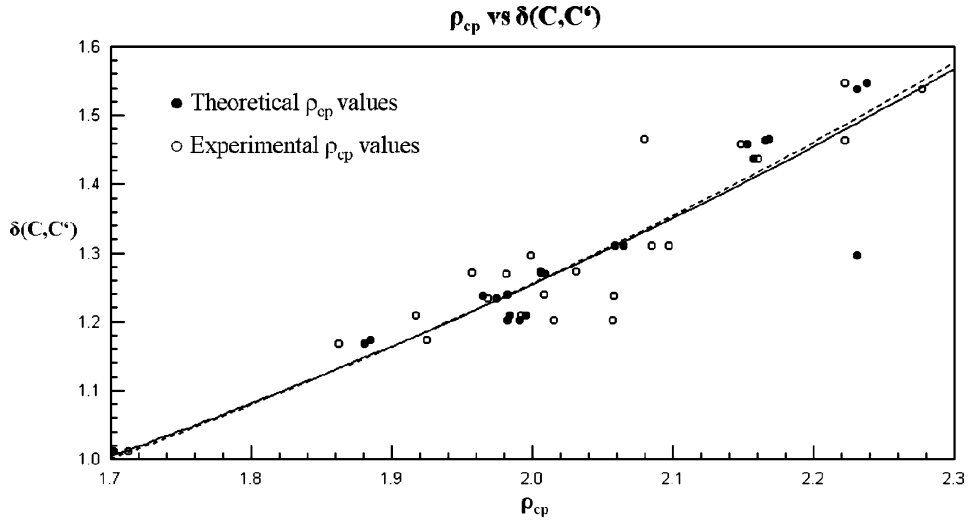

Figure 8. Exponential dependences of ρ_{cp}(eÅ^{-3}) on the theoretical delocalization indices, δ. The R^2 value for the experimental fit (solid line) is 84.3%, and the theoretical (dashed line) R^2 value is 85.1%.

respectively. The theoretical fitting parameters *A* and *B* have values of 0.7434 and 1.6952, respectively. This essentially shows that the bond order increases exponentially as the experimental and theoretical electron densities at the BCP increase, as expected since the greater the bond order the more electrons are associated with the bond.

Conclusions

Experiment and theory shows that the highly twisted nature of helicenes entails the appearance of a weak closed-shell hydrogen−hydrogen (H−H) bonding interaction in the fjord region of the molecule. This H−H bonding closes a 7-membered ring and leads to the appearance of a ring critical point, but the ring system is not distorted enough to entail the splitting of the ring surface and the appearance of a cage critical point as is the case of 1,12-difluorinated derivatives of [4]helicene.[109] The H−H bonding interaction has been characterized topologically according to the quantum theory of atoms in molecules from the experimental and calculated electron densities. Along with this intramolecular H−H bond, several intermolecular interactions have been shown to occur in the crystal. The most important of these are the weak intermolecular H−H bond and three C−H−C van der Waals interactions. These three C−H−C interactions have, simultaneously, some characteristics of a weak hydrogen bonding according to the criteria proposed by Koch and Popelier[78,118] and some characteristics of van der Waals interaction.

The isolated molecule shows that the methyl group donates electronic charge primarily to half the molecule in which it is attached, i.e., rings I and II, and almost no charge from the methyl reaches rings I′ and II′. This is not the case for the experimental data, where a more complex distribution of the charge occurs as a result of the weak intermolecular interactions. Despite the electron enrichment experienced by the substituted side of the ring system at the expense of the methyl group, the distortions induced by the substitution reduce the aromaticity of the substituted ring (I) when compared with the unsubstituted ring (I′). The two internal rings show opposite trends (ring II is slightly more aromatic than II′) and are much less aromatic than the two outer rings. All three aromaticity measures (HOMA, NICS, and θ) give a consistent picture that despite the severe twisting of the molecule it still retains a considerable amount of aromatic character as noted already by Portella et al.[8]

Note Added in Proof. The meaning of QTAIM atomic energies calculated using Kohn−Sham orbitals within the framework of density functional theory has been recently investigated in a paper to appear soon in this journal (Matta, C. F.; Arabi, A. A.; Keith, T. A. *J. Phys. Chem. A* **2007**, *111*, in press).

Acknowledgment. We are indebted to Rigaku/MSC, The Woodlands, TX, for provision of the low-temperature data collection facilities during a Sabbatical Leave Fellowship to T.S.C. We thank the Natural Sciences and Engineering Research Council for Canada for financial support. Finally, we thank Dr. K. N. Robertson and Dr. Parthapratin Munshi for helpful discussions.

Supporting Information Available: CIF file; the final experimental and optimized atomic coordinates, anisotropic displacement parameters, bond distances and angles, multipole population coefficients, κ and κ' values, and residual and static maps obtained from the multipole refinement. This material is available free of charge via the Internet at http://pubs.acs.org.

References and Notes

(1) Harvey, R. G. *Polycyclic Aromatic Hydrocarbons*; John Wiley: New York, 1997.

(2) Garrigues, P.; Lamotte, M. *Polycyclic Aromatic Compouds: Synthesis, Properties, Analytical Measurements, Occurrence and Biological Effects;* Gordon and Breach Science Publishers: Amsterdam, 1993.

(3) Dias, J. R. *Handbook of Polycyclic Hydrocarbons: Part A, Benzenoid Hydrocarbons (Physical Sciences Data, No 30)*; Elsevier: New York, 1987.

(4) Fetzer, J. C. *Large (C>= 24) Polycyclic Aromatic Hydrocarbons: Chemistry and Analysis;* John Wiley: New York, 2000.

(5) Lee, M. L.; Novotny, M. V.; Bartle, K. D. *Analytical Chemistry of Polycyclic Aromatic Compounds;* Academic Press: New York, 1981.

(6) Hites, R. A.; Simonsick, W. J., Jr. *Calculated Molecular Properties of Polycyclic Aromatic Hydrocarbons*; Elsevier: New York, 1987.

(7) Schleyer, P. v. R. G., Ed. *Chem. Rev. (Special Issue: Aromaticity*) **2001**, *101* (5).

(8) Portella, G.; Poater, J.; Bofill, J. M.; Alemany, P.; Solà, M. *J. Org. Chem.* **2005**, *70*, 2509−2521.

(9) Poater, J.; Fradera, X.; Duran, M.; Solà, M. *Chem. Eur. J.* **2003**, *9*, 400−406.

(10) Wiberg, K. B. *J. Org. Chem.* **1997**, *62*, 5720−5727.

(11) Howard, S. T.; Krygowski, T. M. *Can. J. Chem.* **1997**, *75*, 1174−1181.

(12) Suresh, C. H.; Gadre, S. R. *J. Org. Chem.* **1999**, *64*, 2505−2512.

(13) Garratt, P. J. *Aromaticity*; Wiley: New York, 1986.

(14) Clar, E. *The Aromatic Sextet*; John Wiley and Sons Ltd.: London, 1972.
(15) Badger, G. M. *Aromatic Character and Aromaticity*; Cambridge University Press: Cambridge, 1969.
(16) Pullman, A.; Pullman, B. *Adv. Cancer Res.* **1955**, *3*, 117−169.
(17) Neilson, A. H. *PAHs and Related Compounds: Biology*; Springer: New York, 1998.
(18) Luch, A. *The Carcinogenic Effects of Polycyclic Aromatic Hydrocarbons*; Imperial College Press: London, 2005.
(19) Jerina, D. M.; Yagi, H.; Lehr, R. E.; Thakker, D. R.; Schaefer-Ridder, M.; Karle, J. M.; Levin, W. W. A. W.; Chang, R. L.; Cohney, A. H. *Polycyclic Hydrocarbons and Cancer*; Academic Press: New York, 1978; p 173.
(20) Wood, A. W.; Chang, R. L.; Levin, W.; Ryan, D. E.; Thomas, P. E.; Croisy-Delcey, M.; Ittah, Y.; Yagi, H.; Jerina, D. M.; Conney, A. H. *Cancer Res.* **1980**, *40*, 2876−2883.
(21) Wood, A. W.; Chang, R. L.; Levin, W.; Thakker, D. R.; Yagi, H.; Sayer, J. M.; Jerina, D. M.; Conney, A. H. *Cancer Res.* **1984**, *44*, 2320−2324.
(22) Chakravarti, D.; Pelling, J.; Cavalieri, E.; Rogan, E. *Proc. Natl. Acad. Sci. U.S.A.* **1995**, *92*, 10422−10426.
(23) Levin, W.; Wood, A. W.; Chang, R. L.; Ittah, Y.; Croisy-Delcey, M.; Yagi, H.; Jerina, D. M.; Conney, A. H. *Cancer Res.* **1980**, *40*, 3910−3914.
(24) Jerina, D. M.; Sayer, J. M.; Yagi, H.; Croisy-Delcey, M.; Ittah, Y.; Thakker, D. R.; Wood, A. W.; Chang, R. L.; Levin, W.; Conney, A. H. *Adv. Exp. Med. Biol.* **1982**, *136*, 501−523.
(25) Levin, W.; Chang, R. L.; Wood, A. W.; Thakker, D. R.; Yagi, H.; Jerina, D. M.; Conney, A. H. *Cancer Res.* **1986**, *46*, 2257−2261.
(26) Cavalieri, E.; Rogan, E.; Higginbotham, S.; Cremonesi, P.; Salmasi, S. *J. Cancer Res. Clin. Oncol.* **1989**, *115*, 67−72.
(27) Amin, S.; Desai, D.; Dai, W.; Harvey, R. G.; Hecht, S. S. *Carcinogenesis* **1995**, *16*, 2813−2817.
(28) Amin, S.; Desai, D.; el-Bayoumy, K.; Rivenson, A.; Hecht, S. S. *Polycycl. Aromat. Hydrocarbons* **1996**, *11*, 365−371.
(29) Wu, M.; Yan, S.; Patel, D. J.; Geacintov, N. E.; Broyde, S. *Chem. Res. Toxicol.* **2001**, *14*, 1629−1642.
(30) Robertson, K. N. Intermolecular Interactions in a Series of Organoammonium Tetraphenylborates. Ph.D. Thesis; Dalhousie University: Halifax, Canada, 2001.
(31) Matta, C. F.; Hernández-Trujillo, J.; Tang, T. H.; Bader, R. F. W. *Chem. Eur. J.* **2003**, *9*, 1940−1951.
(32) Robertson, K. N.; Knop, O.; Cameron, T. S. *Can. J. Chem.* **2003**, *81*, 727−743.
(33) (a) Matta, C. F. In *Hydrogen Bonding-New Insight, (Challenges and Advances in Computational Chemistry and Physics Series;* Grabowski, S., Ed.; Springer: New York, 2006; Chapter 9, pp 337−375. (b) Hernández-Trujillo, J.; Matta, C. F. *Struct. Chem.* **2007**, in press.
(34) Crabtree, R. H. *Acc. Chem. Res.* **1990**, *23*, 95−101.
(35) Lee, J. C., Jr.; Peris, E.; Rheingold, A. L.; Crabtree, R. H. *J. Am. Chem. Soc.* **1994**, *116*, 11014−11019.
(36) Richardson, T. B.; de Gala, S.; Crabtree, R. H. *J. Am. Chem. Soc.* **1995**, *117*, 12875−12876.
(37) Crabtree, R. H.; Siegbahn, P. E. M.; Eisenstein, O.; Rheingold, A. L.; Koetzle, T. F. *Acc. Chem. Res.* **1996**, *29*, 348−354.
(38) Crabtree, R. H. *Science* **1998**, *282*, 2000−2001.
(39) Klooster, W. T.; Koetzle, T. F.; Siegbahn, P. E. M.; Richardson, T. B.; Crabtree, R. H. *J. Am. Chem. Soc.* **1999**, *121*, 6337−6343.
(40) Popelier, P. L. A. *J. Phys. Chem. A* **1998**, *102*, 1873−1878.
(41) Alkorta, I.; Rozas, I.; Elguero, J. *Chem. Soc. Rev.* **1998**, *27*, 163−170.
(42) Calhorda, M. J. *Chem. Commun.* **2000**, 801−809.
(43) Wojtulewski, S.; Grabowski, S. J. *J. Mol. Struct.* **2003**, *645*, 287−294.
(44) Damodharan, L.; Pattabhi, V. *Tetrahedron Lett.* **2004**, *45*, 9427−9429.
(45) Bodige, S. G.; Sun, D.; Marchand, A. P.; Namboothiri, N. N.; Shukla, R.; Watson, W. H. *J. Chem. Cryst.* **1999**, *29*, 523−530.
(46) Ermer, O.; Mason, S. A. *J. Chem. Soc., Chem. Commun.* **1983**, 53−54.
(47) Grabowski, S. J. *J. Phys. Chem. A* **2000**, *104*, 5551−5557.
(48) Grabowski, S. J. *J. Phys. Chem. A* **2001**, *105*, 10739−10746.
(49) Domagala, M.; Grabowski, S.; Urbaniak, K.; Mloston, G. *J. Phys. Chem. A* **2003**, *107*, 2730−2736.
(50) Wang, C.-C.; Tang, T.-H.; Wu, L.-C.; Wang, Y. *Acta Crystallgr., Sect. A* **2004**, *60*, 488−493.
(51) Grabowski, S. J.; Pfitzner, A.; Zabel, M.; Dubis, A. T.; Palusiak, M. *J. Phys. Chem. B* **2004**, *108*, 1831−1837.
(52) Bacchi, A.; Bosetti, E.; Carcelli, M.; Pelagatti, P.; Rogolini, D. *Eur. J. Inorg. Chem.* **2004**, 1985−1991.
(53) Pozzi, C. G.; Fantoni, A. C.; Goeta, A. E.; Wilson, C. C.; Autino, J. C.; Punte, G. *J. Mol. Struct.* **2005**, *753*, 173−181.
(54) Nemes, G. C.; Silaghi-Dumitrescu, L.; Silaghi-Dumitrescu, I.; Escudié, J.; Ranaivonjatovo, H.; Molloy, K. C.; Mahon, M. F.; Zukerman-Schpector, J. *Organometallics* **2005**, *24*, 1134−1144.
(55) Farrugia, L. J.; Frampton, C. S.; Howard, J. A. K.; Mallinson, P. R.; Peacock, R. D.; Smith, G. T.; Stewart, B. *Acta Crystallogr., Sect. B* **2006**, *62*, 236−244.
(56) Zhurova, E. A.; Tsirelson, V. G.; Zhurov, V. V.; Stash, A. I.; Pinkerton, A. A. *Acta Crystallogr., Sect. B* **2006**, *62*, 513−520.
(57) Zhurova, E. A.; Matta, C. F.; Wu, N.; Zhurov, V. V.; Pinkerton, A. A. *J. Am. Chem. Soc.* **2006**, *128*, 8849−8861.
(58) Cortés-Guzmán, F.; Hernández-Trujillo, J.; Cuevas, G. *J. Phys. Chem. A* **2003**, *107*, 9253−9256.
(59) Montejo, M.; Navarro, A.; Kearley, G. J.; Vázquez, J.; López-González, J. J. *J. Am. Chem. Soc.* **2004**, *126*, 15087−15095.
(60) Glukhov, I. V.; Antipin, M. Y.; Lyssenko, K. A. *Eur. J. Inorg. Chem.* **2004**, 1379−1384.
(61) Glukhov, I. V.; Lyssenko, K. A.; Korlyukov, A. A.; Antipin, M. Y. *Russ. Chem. Bull. Int. Ed.* **2005**, *54*, 547−559.
(62) Vila, A.; Mosquera, R. A. *J. Phys. Chem. A* **2005**, *109*, 6985−6989.
(63) Peña Ruiz, T.; Navarro, A.; Kearley, G. J.; Fernández, Gómez, M. *Chem. Phys.* **2005**, *317*, 159−170.
(64) O'Brien, C. J.; Kantchev, E. A. B.; Chass, G. A.; Hadei, N.; Hopkinson, A. C.; Organ, M. G.; Setiadi, D. H.; Tang, T.-H.; Fang, D.-C. *Tetrahedron* **2005**, *61*, 9723−9735.
(65) Singh, P. C.; Patwari, G. N. *Chem. Phys. Lett.* **2005**, *419*, 265−268.
(66) Singh, P. C.; Patwari, G. N. *Chem. Phys. Lett.* **2005**, *419*, 5−9.
(67) Rzepa, H. S. *Org. Lett.* **2005**, *7*, 4637−4639.
(68) Geier, J.; Rüegger, H.; Grützmacher, H. *Dalton Trans.* **2006**, 129−136.
(69) Freitas, R. F.; Galembeck, S. E. *Chem. Phys. Lett.* **2006**, *423*, 131−137.
(70) Matta, C. F.; Castillo, N.; Boyd, R. J. *J. Phys. Chem. B* **2006**, *110*, 563−578.
(71) Lyssenko, K. A.; Korlyukov, A. A.; Golovanov, D. G.; Ketkov, S. Y.; Antipin, M. Y. *J. Phys. Chem. A* **2006**, *110*, 6545−6551.
(72) Cioslowski, J.; Mixon, S. T. *Can. J. Chem.* **1992**, *70*, 443−449.
(73) Poater, J.; Solà, M.; Bickelhaupt, F. M. *Chem. Eur. J.* **2006**, *12*, 2889−2895.
(74) Bader, R. F. W. *Chem. Eur. J.* **2006**, *12*, 2896−2901.
(75) Bader, R. F. W. *Atoms in Molecules: A Quantum Theory*; Oxford University Press: Oxford, U.K., 1990.
(76) Bader, R. F. W. In *Encyclopedia of Computational Chemistry*; Schleyer P. v. R., Ed.; John Wiley and Sons: Chichester, U.K., 1998; p 64.
(77) Bader, R. F. W.; Nguyen-Dang, T. T. *Adv. Quantum Chem.* **1981**, *14*, 63−124.
(78) Popelier, P. L. A. *Atoms in Molecules: An Introduction*; Prentice Hall: London, 2000.
(79) *The Quantum Theory of Atoms in Molecules: From Solid State to DNA and Drug Design*; Matta, C. F., Boyd, R. J., Eds. Wiley-VCH: Weinheim, 2007.
(80) Bader, R. F. W. *J. Phys. Chem. A* **1998**, *102*, 7314−7323.
(81) Runtz, G. R.; Bader, R. F. W.; Messer, R. R. *Can. J. Chem.* **1977**, *55*, 3040−3045.
(82) Matta, C. F.; Boyd, R. J. In *The Quantum Theory of Atoms in Molecules: From Solid State to DNA and Drug Design*; Matta, C. F., Boyd, R. J., Eds.; Wiley-VCH: Weinheim, 2007; Chapter 1, pp 1−34.
(83) Fradera, X.; Austen, M. A.; Bader, R. F. W. *J. Phys. Chem. A* **1999**, *103*, 304−314.
(84) Poater, J.; Fradera, X.; Duran, M.; Solà, M. *Chem. Eur. J.* **2003**, *9*, 1113−1122.
(85) Matito, E.; Duran, M.; Solà, M. *J. Chem. Phys.* **2005**, *122*, 014109.
(86) Matito, E.; Poater, J.; Solà, M. In *The Quantum Theory of Atoms in Molecules: From Solid State to DNA and Drug Design*; Matta, C. F., Boyd, R. J., Eds.; Wiley-VCH: Weinheim, 2007; Chapter 15, pp 399−423.
(87) Matta, C. F.; Hernández-Trujillo, J. *J. Phys. Chem. A* **2003**, *107*, 7496−7504 (Correction: *J. Phys. Chem A* **2005**, *109*, 10798).
(88) (a) Rigaku Corp. *CrystalClear (CrystalClear Software User's Guide)*; Molecular Structure Corp.: The Woodlands, TX, 1999. (b) Pflugrath, J. W. *Acta Crystallogr., Sect. D* **1999**, *55*, 1718−1725.
(89) Blessing, R. H. *Crystallogr. Rev.* **1987**, *1*, 3−58.
(90) Farrugia, L. J. WinGX (Version 1.64.05). *J. Appl. Crystallogr.* **1999**, *32*, 837−838.
(91) Rigaku and Rigaku/MSC. *CrystalStructure*, Version 3.6.0; Rigaku and Rigaku/MSC: The Woodlands, TX, 2000−2004.
(92) Sheldrick, G. M. *SHELXS97 AND SHELXL97 programs for crystal structure refinement*; University of Gottengen: Gottengen, Germany, 1997.
(93) Farrugia, L. J. *J. Appl. Crystallogr.* **1997**, *30*, 565.
(94) Coppens, P. *X-ray Charge Densities and Chemical Bonding*; Oxford University Press, Inc.: New York, 1997.

(95) Koritsanszky, T. S.; Howard, S.; Macchi, P.; Gatti, C.; Farrugia, L. J.; Mallinson, P. R.; Volkov, A.; Su, Z.; Richter, T.; Hansen, N. K. *XD (version 4.10, July 2003);* Free University of Berlin, Germany; University of Wales, Cardiff, U.K.; Universita di Milano, U.K.; CNR-ISTM, Milano, U.K.; University of Glasgow, U.K.; State University of New York, Buffalo, U.S.A.; University of Nancy, France, 2003.
(96) Su, Z.; Coppens, P. *Acta Crystallogr. Sect. A* **1998**, *54*, 646.
(97) Allen, F. H. *Acta Crystallogr., Sect. B* **1986**, *42*, 512−522.
(98) Semmingsen, D.; Hollander, F. S.; Koetzle, T. F. *J. Chem. Phys.* **1977**, *66*, 4405−4412.
(99) Hirshfeld, F. L. *Acta Crystallogr, Sect. A* **1976**, *32*, 239−244.
(100) Bader, R. F. W. *AIMPAC.* http://www.chemistry.mcmaster.ca/aimpac/.
(101) Biegler-König, F. W.; Bader, R. F. W.; Tang, T.-H. *J. Comput. Chem.* **1982**, *13*, 317−328.
(102) Keith, T. A. (1997). *AIMALL97 (for DOS/Windows).* (Private communication).
(103) Biegler-König, F. W.; Schönbohm, J.; Bayles, D. AIM2000 (http://gauss.fh-bielefeld.de/aim2000).
(104) Biegler-König, F. W.; Schönbohm, J.; Bayles, D. *J. Comput. Chem.* **2001**, *22*, 545−559.
(105) Matta, C. F. *AIMDELOC: Program to calculate AIM localization and delocalization indices (QCPE0802)*; Quantum Chemistry Program Exchange, Indiana University: IN, 2001. (http://qcpe.chem.indiana.edu/).
(106) Schleyer, P. v. R.; Maerker, C.; Dransfeld, A.; Jiao, H.; Hommes, N. J. R. v. E. *J. Am. Chem. Soc.* **1996**, *118*, 6317−6318.
(107) Schleyer, P. v. R.; Manoharan, M.; Wang, Z.-X.; Kiran, B.; Jiao, H.; Puchta, R.; Hommes, N. J. R. v. E. *Org. Lett.* **2001**, *3*, 2465−2468.
(108) Chen, Z.; Wannere, C. S.; Corminboeuf, C.; Puchta, R.; Schleyer, P. v. R. *Chem. Rev.* **2005**, *105*, 3842−3888.
(109) Castillo, N.; Matta, C. F.; Boyd, R. J. *Chem. Phys. Lett.* **2005**, *409*, 265−269.
(110) Matta, C. F.; Castillo, N.; Boyd, R. J. *J. Phys. Chem. A* **2005**, *109*, 3669−3681.
(111) Pauling, L. *The Nature of the Chemical Bond*, 3rd ed.; Cornell University Press: Ithaca, NY, 1960.
(112) Su, Z.; Coppens, P. *Acta Crystallogr., Sect. A* **1992**, *48*, 188−197.
(113) Munshi, P.; Row, T. N. G. *J. Phys. Chem. A* **2005**, *109*, 659−672.
(114) Munshi, P.; Row, T. N. G. *Cryst. Growth Res.* **2006**, *6*, 708−718.
(115) Sykes, P. *A Guidebook to Mechanism in Organic Chemistry*; Longman Group Ltd.: London, 1970.
(116) Kruszewski, J.; Krygowski, T. M. *Tetrahedron Lett.* **1972**, 3842.
(117) Krygowski, T. M. *J. Chem. Inf. Comput. Sci.* **1993**, *33*, 70−78.
(118) Koch, U.; Popelier, P. L. A. *J. Phys. Chem.* **1995**, *99*, 9747−9754.